

Spin Spiral State at a Ferromagnetic Gd Vacuum Interface

Patrick Härtl^{1,*}, Matthias Vogt¹, Markus Leisegang¹, Gustav Bihlmayer², Stefan Blügel², and Matthias Bode^{1,3}

¹Physikalisches Institut, Experimentelle Physik II, Universität Würzburg, Am Hubland, 97074 Würzburg, Germany

²Peter Grünberg Institut and Institute for Advanced Simulation, Forschungszentrum Jülich und JARA, 52425 Jülich, Germany

³Wilhelm Conrad Röntgen-Center for Complex Material Systems (RCCM), Universität Würzburg,

Am Hubland, 97074 Würzburg, Germany



(Received 15 June 2023; revised 20 October 2023; accepted 6 September 2024; published 28 October 2024)

Centrosymmetric bulk magnets made of layered Gd intermetallics had been discovered recently to exhibit helical spin spirals with a wavelength of ≈ 2 nm that transform into skyrmion lattices at certain magnetic fields. Here we report on the observation of a spin spiral state at the Gd(0001) surface. Spin-polarized scanning tunneling microscopy images show striped regions with a periodicity of about 2 nm. These stripes rearrange upon application of an external magnetic field, thereby unambiguously confirming their magnetic origin. Density functional theory calculations explain that competing exchange interactions in the surface layer of Gd(0001) together with a magnetovolume fine-tuning of the exchange interaction to the next Gd layer favor a chiral 2 nm conical spin spiral at the surface, arising as a general behavior of the Gd monolayer.

DOI: [10.1103/PhysRevLett.133.186701](https://doi.org/10.1103/PhysRevLett.133.186701)

Introduction—In the search for skyrmions, fascinating entities that exhibit a range of emergent phenomena [1] and the potential for applications in low-power spintronics [2], recent investigations have led to remarkable discoveries in the field of centrosymmetric Gd/Eu intermetallics. Experiments revealed the presence of spin spiral waves in materials such as Gd₂PdSi₃ [3,4], GdRu₂Si₂ [5], Gd₃Ru₄Al₁₂ [6], EuAl₄ [7,8], or EuGa₂Al₂ [9] that transform into skyrmion lattices under magnetic fields. The periodicities of these spirals and skyrmion lattices are on the nanoscale, i.e., one order of magnitude smaller than those of chiral skyrmions, which are stabilized by the Dzyaloshinskii-Moriya interaction (DMI) [10–12]. They arise from frustrated Ruderman-Kittel-Kasuya-Yosida- (RKKY) type exchange interactions in which competing and distance-dependent ferromagnetic (FM) and antiferromagnetic (AFM) couplings between magnetic ions play a central role [13,14]. Surprisingly, despite the structural and chemical diversity of these materials, the wavelengths of their spin spirals lie within a narrow range, i.e., between 1.9 [5] and 2.8 nm [6], suggesting underlying universal mechanisms.

In the intermetallics, the Gd-Gd interlayer distance is controlled by monatomic Si, Al, Ga, Pd, or Ru spacer layers. Yet, the interlayer distance of a compound can not only be modified by its composition. Also surfaces which interface the bulk with the vacuum generally change the atomic coordination, and thereby the spacing between the surface and the subsurface layer, the electronic structure, and the magnetic interactions.

This raises the question of what happens at the surface of elemental Gd. Gd is a rare-earth metal with a hexagonal close-packed (hcp) crystal structure and a low-temperature easy magnetization axis which is somewhat tilted from the hcp *c* axis [15]. While Gd is FM in the bulk, a variety of unconventional surface magnetic properties have been claimed, including a canted surface magnetization [16], an enhanced surface Curie temperature [17–21], extraordinary phase transitions [19], or an AFM coupling of the topmost layer to the underlying bulk [17]. Yet, other studies report on ordinary surface properties, i.e., a FM surface-bulk coupling and a Curie temperature which is the same for surface and bulk [22–27].

Here we report the observation of a spin spiral state at the surface of epitaxial hcp Gd(0001) films grown on W(110). Experiments are performed at a critical Gd film thickness of $\Theta_{\text{crit}} \approx (100 \pm 20)$ atomic layers (AL), where a spin reorientation transition (SRT) from in-plane to out-of-plane takes place [28,29]. By making use of high-resolution spin-polarized (SP)-STM, we identify striped regions with a periodicity of again ≈ 2 nm. Their magnetic origin is verified by a field-induced rearrangement. Density functional theory (DFT) calculations suggest that the reduction of the Gd coordination number from bulk over the surface to the layered intermetallics introduces modifications to the Fermi surface. This triggers competing exchange interactions within the surface layer which are only marginally affected by interlayer interactions and result in a conical spin spiral (CSS) with a periodicity of 2 nm. Our data reveal that the CSS appears at the surface when the magnetic interactions get locally modified, e.g., due to strain or adsorbates.

*Contact author: patrick.haertl@uni-wuerzburg.de

Experimental setup—Experiments were performed under ultrahigh vacuum conditions ($p \leq 5 \times 10^{-11}$ mbar). Preparation details can be found in Refs. [29,30]. STM measurements were performed in the constant-current mode at a temperature $T_{\text{STM}} \approx 4.5$ K. The bias voltage U is applied to the sample. A magnetic field $|\mu_0 H| \leq 3$ T along the surface normal can be applied. For magnetically sensitive SP-STM measurements, the W tip was dipped into Gd or gently pulsed at $U \geq \pm 4$ V, resulting in a tip magnetization which is canted relative to the Gd surface. dI/dU maps were obtained by lock-in technique. For better visibility of our STM data, the z signal was augmented by its derivative, dz/dx [29].

Experimental results—Figure 1(a) shows the topography and Fig. 1(b) the magnetically sensitive dI/dU map of a Gd film with a thickness $\Theta_{\text{crit}} \approx (100 \pm 20)$ AL just at the SRT from in-plane to out-of-plane. To fully comprehend the magnetic structure displayed in Fig. 1(b), some background about the thickness-dependent domain structure of Gd/W(110) is required.

While large in-plane domains exist at $\Theta < \Theta_{\text{crit}}$ [29], stripe domains with an alternating predominantly upward and downward pointing magnetization were observed for $\Theta > \Theta_{\text{crit}}$. This SRT can be explained by a competition between magnetostatic and magnetocrystalline contributions to the anisotropy energy. At low film thickness an in-plane magnetization is favored since a magnetization along the surface normal would cause a large magnetostatic energy penalty. Yet, since the magnetocrystalline anisotropy energy increases with film thickness, it dominates above Θ_{crit} and the film adopts an out-of-plane easy axis.

The overview magnetic dI/dU map of Fig. 1(b) shows that the nucleation of stripe domains occurs inhomogeneously, i.e., in some patches only, whereas the surrounding regions exhibit no specific contrast [31]. This is a reassuring indication that we are in the vicinity of the SRT, caused by the cancellation of the magnetocrystalline and the magnetostatic anisotropy which makes the film highly susceptible to competing ordering phenomena [32]. Indeed, the high-resolution scan of the region within the black box in Fig. 1(b) reveals stripes oriented along one Gd $\langle \bar{1}100 \rangle$ direction [33]; see Fig. 1(c). Line profiles show typical periodicities of 1.9–2.2 nm; see Fig. 1(d). As we will derive theoretically below, these stripes originate from a CSS state at a magnet’s vacuum interface.

To verify the magnetic origin of these stripes, we performed field-dependent SP-STM measurements, see Fig. 2 and Ref. [34], Sec. III, for details. The first image, Fig. 2(a), has been recorded in an external field $\mu_0 H = -200$ mT. We find two regions (indicated by blue loops) that exhibit stripes with a periodicity of ≈ 2 nm. While the stripes in region (1) are oriented parallel to the [001] direction of the underlying W(110) substrate, they are rotated by 60° in region (2). As the field is raised to

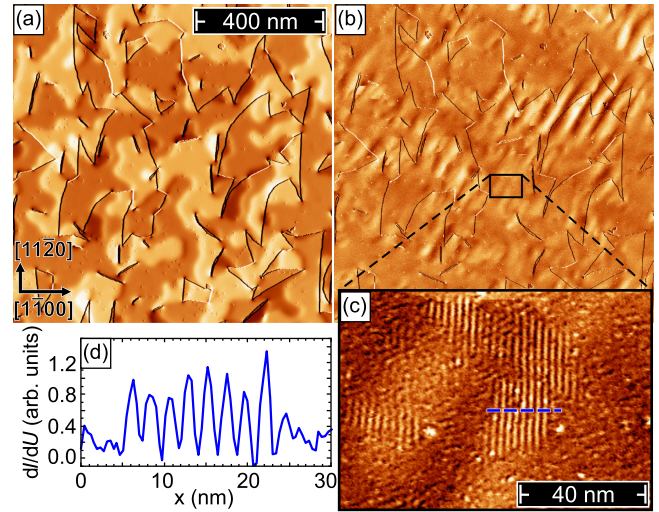


FIG. 1. (a) STM topography image of an 80 AL Gd(0001) film on W(110). (b) Magnetically sensitive dI/dU map obtained with a Gd/W tip. In some areas the nucleation of stripe domains is observed, indicating the SRT from in-plane to out-of-plane. The surrounding Gd surface appears featureless. (c) The higher-resolution scan taken within the box in (b) reveals that some regions exhibit periodic stripes. (d) Line section measured along the hatched blue line in (c). The stripe periodicity amounts to ≈ 2 nm.

-100 mT, Fig. 2(b), weak stripes (marked by two blue arrows) on the left-hand side just outside region (1) extend and become more pronounced. When the field is changed to $+100$ mT, Fig. 2(c), the stripe orientation in (1) rotates by 60° ; see Fig. 2(d). Furthermore, the nucleation of additional stripes just below and left of region (2) can be observed. At $+200$ mT some stripes in (2) also rotate, see blue arrows in Fig. 2(e). Since some stripes remain unchanged we can exclude that the tip’s magnetization direction is influenced by the external field.

Interestingly, the changes appear to be fully reversible. The data presented in Figs. 2(f)–2(i) show dI/dU maps of the same region, but now when the magnetic field is reduced from $+100$ mT back to -200 mT, respectively. Within the signal-to-noise ratio available here, the data taken at the end of the hysteresis, Fig. 2(i), are virtually indistinguishable from the initial situation, Fig. 2(a).

Calculations—To obtain material specific parameters, we performed DFT calculations of a relaxed 10 layer and an unsupported monolayer hcp Gd(0001) film in the generalized gradient approximation [35] with a typical Hubbard $U = 6.7$ eV, $J = 0.7$ eV [36], an electronic temperature of 316 K, and a lattice constant of 3.636 Å. We use the full-potential linearized augmented plane wave code FLEUR [37] to estimate the exchange interactions. Spin spiral calculations are performed using the generalized Bloch theorem, where spin-orbit coupling (SOC) is included in first order perturbation theory [38]. To explore the magnetic phase diagram, where analytic solutions cannot be obtained, we use the spin-dynamics package SPIRIT [43].

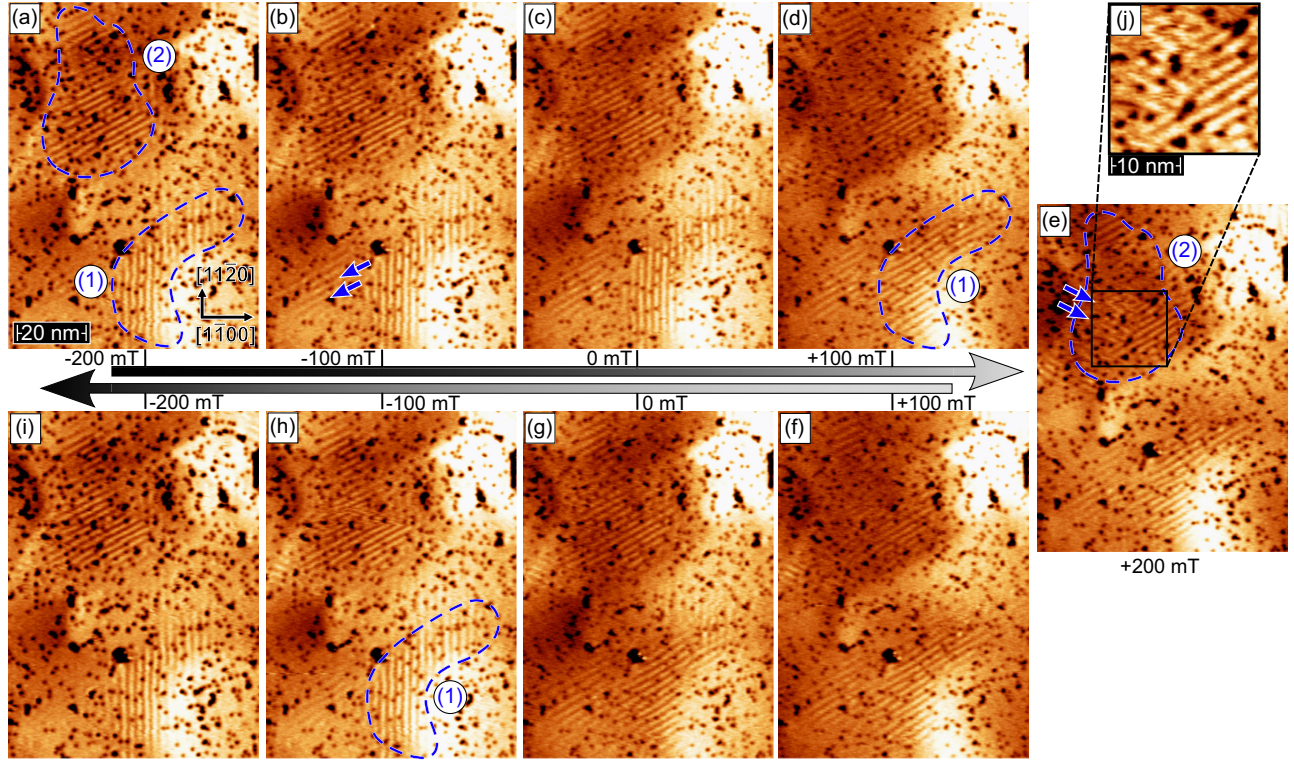


FIG. 2. Magnetic field-dependent series of SP-STM images of a Gd(0001) surface area where two striped regions can be recognized, indicated by blue loops (1) and (2). (a) $\mu_0 H = -200$ mT, (b) -100 mT, (c) 0 mT, (d) $+100$ mT, (e) $+200$ mT, (f) $+100$ mT, (g) 0 mT, (h) -100 mT, and (i) -200 mT. Several field-induced changes of the stripe pattern can be observed, such as the extension of striped regions, see arrow in (b), or a changing stripe orientation, see loops in (a), (d), (e), and (h). See Ref. [34] for details.

Theoretical results—On the basis of a minimal atomistic spin model, we explore under which conditions a CSS forms in the surface layer and how the cone angle and the wave vector of the spiral depend on the DFT-derived magnetic interaction parameters. An elemental in-plane-oriented FM film with layers $j = 0, 1, \dots$ ($j = 0$ being the surface layer) and atomic sites $i = 0, 1, \dots$ in each layer is considered. The easy axis of magnetization defines the x direction and the surface normal is along z . The CSS, if present, propagates with a wave vector $\mathbf{q} = [\bar{1}100]$ in the y direction. The magnetic moments of size S of the atoms i in layer j (position $\mathbf{R}_{i,j}$) are then written as

$$\mathbf{S}_{i,j} = S(\cos \vartheta_j, \sin \vartheta_j \sin \varphi_{i,j}, -\sin \vartheta_j \cos \varphi_{i,j}), \quad (1)$$

where $\varphi_{i,j} = \mathbf{q} \cdot \mathbf{R}_{i,j}$ denotes the phase and ϑ_j the cone angle, i.e., the opening angle of the conical spiral. The nearest-neighbor Heisenberg-type in-plane exchange interaction is denoted as $J_{j,\parallel}^{(1)}$ while the interaction between layers j and $j + 1$ is called $J_{j,\perp}$. In each layer also a second-nearest-neighbor exchange $J_{j,\parallel}^{(2)}$ is taken into account to model the competition between FM and AFM exchange leading to exchange frustration. The nearest-neighbor DMI is denoted \mathbf{D}_j . In addition, it must be considered that a CSS

has to overcome a magnetic anisotropy $\bar{K} \sin^2 \vartheta_j$, where \bar{K} is the average of the anisotropies in the hard and medium axis [12].

In a first approximation, all nearest-neighbor exchange constants are set, $J_{j,\parallel}^{(1)} = J_{j,\perp} = J$, and assumed to be FM ($J > 0$). $J_{j,\parallel}^{(2)}$ and \mathbf{D} are included only in the first layer (justification will be obtained from DFT) and reduced quantities $\tilde{J}^{(2)} = J_{j,\parallel}^{(2)}/J$, $\tilde{D} = D/J$, and $\tilde{K} = \bar{K}/J$ are used. Films of finite thickness are considered, whereby FM order for the central layers is assured by large J constants. The results from spin-dynamics calculations are shown in Fig. 3 [34]. Evidently, large negative, i.e., AFM exchange values of $\tilde{J}^{(2)}$, or large spiralization values \tilde{D} are necessary to form a CSS at the surface. Spiral formation (with smaller cone angles) in deeper layers or reducing \tilde{K} lowers these values a bit (see Fig. 3).

In the next step, parameters are explored by DFT [34]. To obtain $J_{0,\parallel}$, spin spiral calculations with $\vartheta_0 = \pi/2$ and $\vartheta_{j>0} = 0$ are performed. D_0^{\parallel} is extracted from calculations including SOC. The results are shown in Fig. 4(a) for $\mathbf{q} \parallel [\bar{1}100]$: without SOC an energy minimum of -5.8 meV at $\mathbf{q} = 0.34 \text{ \AA}^{-1}$ is obtained, corresponding to a wavelength of 1.9 nm. From a fit we obtain $J_{0,\parallel}^{(1)} = 20.4$ meV and $J_{0,\parallel}^{(2)} = -10.5$ meV. Their different sign denotes a

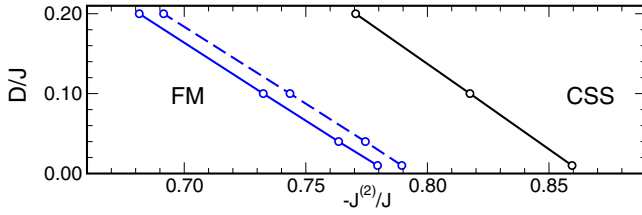


FIG. 3. Phase diagram with the stability regions for FM and CSS solutions for a 6 layer film obtained from spin-dynamics simulations. The black line is obtained when the lowest 5 layers are kept FM using $J_{\parallel} = J_{\perp} = 9J$, the blue lines when only the lowest 2 layers are fixed this way, while in the second to fourth layer $J_{\parallel} = J_{\perp} = J$. Full (broken) lines are phase boundaries with $\bar{K} = 0.01$ ($\bar{K} = 0.05$).

competing interaction and their ratio, -0.51 , is surprisingly large, but not large enough to obtain a CSS without DMI. The energy contribution by the DMI is ≈ 1.6 meV, and we obtain $\bar{D} = D_{0\parallel}^{\parallel}/J_{0\parallel}^{(1)} = 0.06$. These parameters locate the system on the FM side in Fig. 3. To analyze the exchange interactions in the second layer, the calculations were repeated with $\vartheta_0 = \vartheta_1 = \pi/2$ and $\vartheta_{j>1} = 0$. Comparison to the former calculations gives $J_{1\parallel}^{(1)} = 19.1$ meV and $J_{1\parallel}^{(2)} = -4.4$ meV. In addition, $J_{0\perp} = 14$ meV and $J_{1\perp} = 11.5$ meV can be extracted.

Using these parameters, a spin-dynamics calculation of a six layer hcp film with two fixed FM central layers was performed. Still, the solution is FM also in the topmost layer. If, however, the exchange parameters $J_{0\parallel}^{(1)}$ and $J_{0\perp}$ are artificially reduced to $J_{1\parallel}^{(1)}$ and $J_{1\perp}$, i.e., by 6% and 18%, respectively, a CSS in the topmost layer (and a bit extending to the subsurface layer) appears; see inset of Fig. 4 herein and Fig. S12 in [34]. The source of such a reduction could be, e.g., the strong sensitivity of J on the lattice constant and the c/a ratio [44], which may be modified by epitaxial strain, but also by the choice of the exchange correlation functional or the value of the Hubbard U . In conclusion, the conditions for the formation of the CSS are in close reach.

Discussion—Given the good agreement between the experimentally observed periodicity of the magnetic stripe pattern and the wavelength obtained by DFT, we conclude that Gd(0001) films grown on W(110) with a thickness just at the SRT tend to form a CSS. While the formation is suppressed by the magnetic anisotropy below and above Θ_{crit} , the film becomes highly susceptible to competing exchange interactions in the Gd surface layer when the various anisotropies cancel at Θ_{crit} . This delicate balance manifests itself by the experimentally observed local character of the CSS, cf. Fig. 1(a). It might result from mesoscopic strain caused by the film’s complex structural properties combined with the strong magnetovolume effect of Gd, that cannot be fully accounted for in DFT, potentially explaining the diverse spectrum of inconsistent experimental results [16–21].

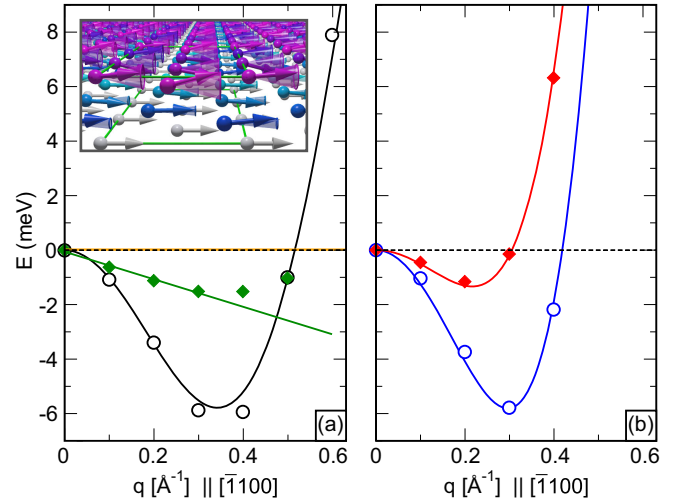


FIG. 4. Total energy without SOC (empty circles) of a flat spin spiral as function of \mathbf{q} in $[\bar{1}100]$ direction induced in (a) the surface layer of a 10 layer Gd(0001) film and (b) an unsupported monolayer. Solid lines are fits to calculated points determining $J^{(1)}$ and $J^{(2)}$. The green line is a linear fit to the first four data points (green diamonds) containing the SOC. Its slope determines the DMI D_0 . \bar{K} is tiny and marked by an orange line (data taken from [45]). Inset: schematic representation of the CSS showing the first three Gd layers. The opening angle of the CSS is largest at the topmost layer and weakly extends to the second layer. The magnetic unit cell is indicated by green rectangles. (b) Calculations for electronic temperatures of 316 K (blue circles) and 1052 K (red diamonds) indicate the role of the Fermi surface.

We propose that the intriguing observation of an order of 2 nm spin spiral wave formation, consistently observed in all skyrmion-forming Gd intermetallics and for the Gd surface, is inherently tied to the two-dimensional nature of the Gd layer within these compounds. To substantiate this conjecture, we adopt a drastic approximation, evaluating the total energy of spin spiral states as function of the \mathbf{q} vector for an unsupported Gd(0001) monolayer sharing the same lattice constant as bulk Gd. Our findings for two electronic temperatures, depicted in Fig. 4(b), reveal a spin spiral ground state along the $[\bar{1}100]$ direction with a weakly temperature-dependent pitch and a temperature-dependent energy gain. The pitch varies from 2.1 nm at low (blue line, 316 K) to 2.9 nm at high electronic temperature (red line, 1052 K). The strong dependence of the energy gain on the electronic temperature prescribed by the Fermi-Dirac distribution for electron-hole excitations evidences that the competing exchange interaction is a consequence of the two-dimensional Fermi surface with its fundamental link to a strong RKKY mechanism [13].

Summary—In summary, we observed the local formations of magnetic stripes with a 2 nm periodicity at the Gd(0001) surface by SP-STM. DFT reveals a relatively large ratio of the AFM next-nearest to FM nearest-neighbor coupling, also favoring a 2 nm spin spiral. Our results

indicate that the coupling to the bulk is overcome by local modifications of the magnetic properties, e.g., due to strain caused by the underlying substrate. The conical spin spiral becomes a precursor of the skyrmion lattice if the magnetic field is strong enough to unwind the spiral. Reducing the competition of the external field and the exchange field from the Gd bulk motivates the design of artificial Gd intermetallics, e.g., Gd|Y|Gd bulk or Gd|RuAl|Gd bulk, where the thickness of the interlayers can be optimized for the nucleation of exchange-stabilized skyrmions. Gd forms layered centrosymmetric ternary intermetallics with propensity for AFM order [13] that belong to 13 crystal families. We speculate that many of those will exhibit spin spiral waves and skyrmions of 2 nm pitch at bulk and surface.

Acknowledgments—S. B. thanks Juba Bouaziz for fruitful discussions. We acknowledge financial support by the Deutsche Forschungsgemeinschaft (DFG, German Research Foundation), S. B. through SFB 1238 Project No. 277146847 (project C01), M. B. through Project No. 510676484 (GZ: BO 1468/29-1), and under Germany's Excellence Strategy through the Würzburg–Dresden Cluster of Excellence on Complexity and Topology in Quantum Matter—ct.qmat (EXC 2147, Project No. 390858490). G. B. gratefully acknowledges computing time granted through JARA-HPC on the supercomputer JURECA at Forschungszentrum Jülich.

- [1] A. Neubauer, C. Pfleiderer, B. Binz, A. Rosch, R. Ritz, P. G. Niklowitz, and P. Böni, Topological Hall effect in the A phase of MnSi, *Phys. Rev. Lett.* **102**, 186602 (2009).
- [2] A. Fert, N. Reyren, and V. Cros, Magnetic skyrmions: Advances in physics and potential applications, *Nat. Rev. Mater.* **2**, 17031 (2017).
- [3] T. Kurumaji, T. Nakajima, M. Hirschberger, A. Kikkawa, Y. Yamasaki, H. Sagayama, H. Nakao, Y. Taguchi, T. Arima, and Y. Tokura, Skyrmion lattice with a giant topological Hall effect in a frustrated triangular-lattice magnet, *Science* **365**, 914 (2019).
- [4] J. A. M. Paddison, B. K. Rai, A. F. May, S. Calder, M. B. Stone, M. D. Frontzek, and A. D. Christianson, Magnetic interactions of the centrosymmetric skyrmion material Gd₂PdSi₃, *Phys. Rev. Lett.* **129**, 137202 (2022).
- [5] N. D. Khanh, T. Nakajima, X. Yu, S. Gao, K. Shibata, M. Hirschberger, Y. Yamasaki, H. Sagayama, H. Nakao, L. Peng, K. Nakajima, R. Takagi, T. Arima, Y. Tokura, and S. Seki, Nanometric square skyrmion lattice in a centrosymmetric tetragonal magnet, *Nat. Nanotechnol.* **15**, 444 (2020).
- [6] M. Hirschberger, T. Nakajima, S. Gao, L. Peng, A. Kikkawa, T. Kurumaji, M. Kriener, Y. Yamasaki, H. Sagayama, H. Nakao, K. Ohishi, K. Kakurai, Y. Taguchi, X. Yu, T. Arima, and Y. Tokura, Skyrmion phase and competing magnetic orders on a breathing kagomé lattice, *Nat. Commun.* **10**, 5831 (2019).
- [7] R. Takagi, N. Matsuyama, V. Ukleev, L. Yu, J. S. White, S. Francoual, J. R. L. Mardegan, S. Hayami, H. Saito, K. Kaneko, K. Ohishi, Y. Ōnuki, T. Arima, Y. Tokura, T. Nakajima, and S. Seki, Square and rhombic lattices of magnetic skyrmions in a centrosymmetric binary compound, *Nat. Commun.* **13**, 1472 (2022).
- [8] H. Miao, J. Bouaziz, G. Fabbris, W. R. Meier, F. Z. Yang, H. X. Li, C. Nelson, E. Vescovo, S. Zhang, A. D. Christianson, H. N. Lee, Y. Zhang, C. D. Batista, and S. Blügel, Spontaneous chirality flipping in an orthogonal spin-charge ordered topological magnet, *Phys. Rev. X* **14**, 011053 (2024).
- [9] J. M. Moya *et al.*, Incommensurate magnetic orders and topological Hall effect in the square-net centrosymmetric EuGa₂Al₂ system, *Phys. Rev. Mater.* **6**, 074201 (2022).
- [10] I. E. Dzyaloshinskii, Thermodynamic theory of “weak” ferromagnetism in antiferromagnetic substances, *Sov. Phys. JETP* **5**, 1259 (1957), <http://jetp.ras.ru/cgi-bin/e/index/e/5/6/p1259?a=list>.
- [11] T. Moriya, Anisotropic superexchange interaction and weak ferromagnetism, *Phys. Rev.* **120**, 91 (1960).
- [12] M. Bode, M. Heide, K. von Bergmann, P. Ferriani, S. Heinze, G. Bihlmayer, A. Kubetzka, O. Pietzsch, S. Blügel, and R. Wiesendanger, Chiral magnetic order at surfaces driven by inversion asymmetry, *Nature (London)* **447**, 190 (2007).
- [13] J. Bouaziz, E. Mendive-Tapia, S. Blügel, and J. B. Staunton, Fermi-surface origin of skyrmion lattices in centrosymmetric rare-earth intermetallics, *Phys. Rev. Lett.* **128**, 157206 (2022).
- [14] T. Nomoto and R. Arita, *Ab initio* exploration of short-pitch skyrmion materials: Role of orbital frustration, *J. Appl. Phys.* **133**, 150901 (2023).
- [15] J. J. M. Franse and R. Gersdorf, Magnetic anisotropy of Gd metal at 4 K under pressure, *Phys. Rev. Lett.* **45**, 50 (1980).
- [16] D. Li, J. Zhang, P. A. Dowben, K. Garrison, P. D. Johnson, H. Tang, T. G. Walker, H. Hopster, J. C. Scott, D. Weiler *et al.*, Canted magnetic moments at the Gd (0001) surface, *MRS Online Proc. Libr.* **313**, 451 (1993).
- [17] D. Weller, S. F. Alvarado, W. Gudat, K. Schröder, and M. Campagna, Observation of surface-enhanced magnetic order and magnetic surface reconstruction on Gd(0001), *Phys. Rev. Lett.* **54**, 1555 (1985).
- [18] D. Weller and S. F. Alvarado, Preparation of remanently ferromagnetic Gd(0001), *J. Appl. Phys.* **59**, 2908 (1986).
- [19] E. Vescovo, C. Carbone, and O. Rader, Surface magnetism of Gd(0001) films: Evidence for an unexpected phase transition, *Phys. Rev. B* **48**, 7731 (1993).
- [20] D. Li, J. Pearson, S. D. Bader, D. N. McIlroy, C. Waldfried, and P. A. Dowben, Spin polarization of the conduction bands and secondary electrons of Gd(0001), *J. Appl. Phys.* **79**, 5838 (1996).
- [21] E. D. Tober, F. J. Palomares, R. X. Ynzunza, R. Denecke, J. Morais, Z. Wang, G. Bino, J. Liesegang, Z. Hussain, and C. S. Fadley, Observation of a ferromagnetic-to-paramagnetic phase transition on a ferromagnetic surface using spin-polarized photoelectron diffraction: Gd(0001), *Phys. Rev. Lett.* **81**, 2360 (1998).
- [22] A. Aspelmeier, F. Gerhardter, and K. Baberschke, Magnetism and structure of ultrathin Gd films, *J. Magn. Magn. Mater.* **132**, 22 (1994).

- [23] A. Berger, A. W. Pang, and H. Hopster, Magnetic reorientation transition of Gd(0001)/W(110) films, *Phys. Rev. B* **52**, 1078 (1995).
- [24] M. Donath, B. Gubanka, and F. Passek, Temperature-dependent spin polarization of magnetic surface state at Gd(0001), *Phys. Rev. Lett.* **77**, 5138 (1996).
- [25] M. Getzlaff, M. Bode, S. Heinze, R. Pascal, and R. Wiesendanger, Temperature-dependent exchange splitting of the magnetic Gd(0001) surface state, *J. Magn. Magn. Mater.* **184**, 155 (1998).
- [26] O. Zeybek, N. P. Tucker, S. D. Barrett, and E. A. Seddon, High-resolution secondary electron spin-polarisation from gadolinium, *J. Magn. Magn. Mater.* **198–199**, 674 (1999).
- [27] C. S. Arnold and D. P. Pappas, Gd(0001): A semi-infinite three-dimensional Heisenberg ferromagnet with ordinary surface transition, *Phys. Rev. Lett.* **85**, 5202 (2000).
- [28] A. Berger, A. W. Pang, and H. Hopster, Magnetic reorientation transition in epitaxial Gd-films, *J. Magn. Magn. Mater.* **137**, L1 (1994).
- [29] P. Härtl, M. Leisegang, and M. Bode, Magnetic domain structure of epitaxial Gd films grown on W(110), *Phys. Rev. B* **105**, 174431 (2022).
- [30] Kh. Zakeri, T. R. F. Peixoto, Y. Zhang, J. Prokop, and J. Kirschner, On the preparation of clean tungsten single crystals, *Surf. Sci.* **604**, L1 (2010).
- [31] C. Won, Y. Z. Wu, J. Choi, W. Kim, A. Scholl, A. Doran, T. Owens, J. Wu, X. F. Jin, H. W. Zhao, and Z. Q. Qiu, Magnetic stripe melting at the spin reorientation transition in Fe/Ni/Cu(001), *Phys. Rev. B* **71**, 224429 (2005).
- [32] The magnetic stripes are not limited to the SRT but occur within approximately ± 20 AL around it. In 80 AL or 120 AL Gd(0001) films, we observe stripes with a periodicity of about 2 nm. These films show both in-plane and out-of-plane domains. We assume that, due to the thickness of the film near the SRT, remaining anisotropies are sufficiently weak to permit the formation of surface spin spiral configurations; see Ref. [34].
- [33] Although a single stripe direction dominates in the scanned area shown here, data presented in Ref. [34] confirm that stripes oriented along all three Gd axes can be found with equal probability.
- [34] See Supplemental Material at <http://link.aps.org/supplemental/10.1103/PhysRevLett.133.186701> for a detailed analysis of the SRT range, verification of the in-plane ferromagnetic domains, and detailed information on the simplified model and DFT calculations, which includes Refs. [29,35–42].
- [35] J. P. Perdew, K. Burke, and M. Ernzerhof, Generalized gradient approximation made simple, *Phys. Rev. Lett.* **77**, 3865 (1996).
- [36] Ph. Kurz, G. Bihlmayer, and S. Blügel, Magnetism and electronic structure of hcp Gd and the Gd(0001) surface, *J. Phys. Condens. Matter* **14**, 6353 (2002).
- [37] Ph. Kurz, F. Förster, L. Nordström, G. Bihlmayer, and S. Blügel, *Ab initio* treatment of noncollinear magnets with the full-potential linearized augmented plane wave method, *Phys. Rev. B* **69**, 024415 (2004).
- [38] M. Heide, G. Bihlmayer, and S. Blügel, Describing Dzyaloshinskii-Moriya spirals from first principles, *Physica (Amsterdam)* **404B**, 2678 (2009).
- [39] M. Bode, O. Pietzsch, A. Kubetzka, S. Heinze, and R. Wiesendanger, Experimental evidence for intra-atomic non-collinear magnetism at thin film probe tips, *Phys. Rev. Lett.* **86**, 2142 (2001).
- [40] K. von Bergmann, M. Menzel, D. Serrate, Y. Yoshida, S. Schröder, P. Ferriani, A. Kubetzka, R. Wiesendanger, and S. Heinze, Tunneling anisotropic magnetoresistance on the atomic scale, *Phys. Rev. B* **86**, 134422 (2012).
- [41] S. Krause, L. Berbil-Bautista, G. Herzog, M. Bode, and R. Wiesendanger, Current-induced magnetization switching with a spin-polarized scanning tunneling microscope, *Science* **317**, 1537 (2007).
- [42] S. Abdelouahed and M. Alouani, Magnetic anisotropy in Gd, GdN, and GdFe₂ tuned by the energy of gadolinium 4*f* states, *Phys. Rev. B* **79**, 054406 (2009).
- [43] G. P. Müller, M. Hoffmann, C. Dißelkamp, D. Schürhoff, S. Mavros, M. Sallermann, N. S. Kiselev, H. Jónsson, and S. Blügel, *Spirit*: Multifunctional framework for atomistic spin simulations, *Phys. Rev. B* **99**, 224414 (2019).
- [44] I. Turek, J. Kudrnosvský, G. Bihlmayer, and S. Blügel, *Ab initio* theory of the exchange interactions and Curie temperature of bulk Gd, *J. Phys. Condens. Matter* **15**, 2771 (2003).
- [45] M. Colarieti-Tosti, T. Burkert, O. Eriksson, L. Nordström, and M. S. S. Brooks, Theory of the temperature dependence of the easy axis of magnetization in hcp Gd, *Phys. Rev. B* **72**, 094423 (2005).